Earthquake Geotechnical Engineering for Protection and Development of Environment and Constructions – Silvestri & Moraci (Eds)
© 2019 Associazione Geotecnica Italiana, Rome, Italy, ISBN 978-0-367-14328-2

A simple constitutive model for taking into account soil nonlinearity and strength in 1D site response analyses

R. Conti
Università di Roma Niccolò Cusano, Rome, Italy

V. Licata
Anas S.p.A., Rome, Italy

M. Angelini
TechnipFMC, Rome, Italy

ABSTRACT: One of the main issues when performing site response analyses in the design practice consists in finding a compromise between the often limited availability of site-specific experimental data to characterize the cyclic soil behaviour and the necessity of a proper constitutive representation of such behaviour, including nonlinearity, hysteresis and strength. This paper presents a new 1D nonlinear soil model, capable of describing such features with a simple and easy to calibrate constitutive equation. The basic idea of the proposed model consists in linking the nonlinear behaviour of the soil to its small strain stiffness and shear strength. In this way, the model parameters can be significantly reduced, without losing accuracy in the characterization of those features relevant in site response analyses, such as the dependence of nonlinear soil properties on plasticity index and confining pressure. It is shown that the proposed model provides a good description of the soil behaviour, for both sands and clays, in the whole strain range. Moreover, it is demonstrated that an erroneous prediction of the soil shear strength can lead to a misinterpretation of the amplification phenomena within the soil deposit, together with a possible gross underestimation of the actual accelerations at surface.

1 INTRODUCTION

Seismic site response analysis is the primary step in many applications of earthquake engineering. To this end, various approaches can be used, characterized by different degrees of approximation. The most common approach consists of evaluating the effects of local stratigraphic conditions on the earthquake-induced ground motion at surface by means of one-dimensional vertical propagation of SH waves through horizontal soil layers. In this context, the constitutive model for the soil can be reduced to a scalar equation between the shear stress, τ, and the shear strain, γ.

Site response analyses are typically affected by many sources of uncertainties. Among these: (i) the definition of the input rock motion; (ii) the identification and characterization of the soil profile; (iii) the one-dimensional representation of the soil domain; (iv) the adoption of appropriate methods of analysis and constitutive soil models.

Based on the above considerations, it is clear that, when performing this type of analysis in the design practice, one of the major issues consists in finding a compromise between the often limited availability of site-specific experimental data to characterize the cyclic soil behaviour and the necessity of a proper constitutive representation of such behaviour, including nonlinearity, hysteresis and strength. Moreover, nonlinear soil properties should be defined as a function of depth and consistent with site-specific shear wave velocity and strength profiles (Régnier *et al.*, 2018).

Summarizing, a crucial point in standard design practice is to handle a minimum number of constitutive parameters, consistently with the limited availability of site-specific information, but retaining a proper representation of the cyclic soil behaviour. This paper presents two

simple constitutive soil models, capable of describing all the above features with simple and easy to calibrate constitutive equations.

2 SOIL BEHAVIOUR UNDER CYCLIC LOADINGS

2.1 *Experimental observations*

The nonlinear and dissipative behaviour of geomaterials under cyclic loadings can be described synthetically by means of four key ingredients: (i) the maximum shear modulus, G_0; (ii) the secant shear modulus degradation curve, $G/G_0(\gamma)$; (iii) the damping curve, $D(\gamma)$; and (iv) the shear strength, τ_{lim}.

As far as the $G/G_0(\gamma)$ and $D(\gamma)$ curves are concerned, which control the soil behaviour in the small-to-medium strain range, the main factors affecting nonlinearity and hysteresis of soils are the mean effective stress, p', and the plasticity index, PI.

As far as the soil shear strength is concerned, τ_{lim} has two relevant effects in seismic site response analyses. On the one hand, it imposes a physical constraint to the maximum shear stress that can be applied to a soil layer during the earthquake and, then, to the maximum acceleration that can propagate through the soil deposit. On the other hand, it affects the nonlinear properties of the soil in the medium strain range. As a matter of fact, experimental observations have shown that the effects of p' and PI on G/G_0 are correlated with those on G_0 and τ_{lim} (Kishida, 2017).

2.2 *Constitutive considerations: The role of* τ_{lim}

To have a better understanding of the dual role of τ_{lim} in governing the cyclic behaviour of soils under medium-to-large strains, and of how to include such evidences in a simple constitutive equation, the classical hyperbolic model can be used as an example. In this case, the backbone curve can be written in scalar form as $\tau(\gamma) = \Phi(\gamma)$, where $\Phi(\gamma)$ is given by:

$$\Phi(\gamma) = \frac{G_0\gamma}{1 + \left|\frac{\gamma}{\gamma_{ref}}\right|} \tag{1}$$

where $\gamma_{\text{ref}} = \tau_{\text{lim}}/G_0$ is the reference shear strain, as originally defined by Kondner and Zelasko (1963). Eq. (1) guarantees a finite value of the soil shear strength, even though asymptotically for $\gamma \to \infty$. The corresponding shear modulus degradation curve is:

$$G/G_0(\gamma) = \frac{1}{1 + \frac{\gamma}{\gamma_{ref}}} \tag{2}$$

According to Eq.(2), τ_{lim} and G_0 govern the $G/G_0(\gamma)$ curve (and indirectly the $D(\gamma)$ curve) through their ratio γ_{ref}. Taking into account that $\tau_{lim} \propto p'$ and $G_0 \propto p'^n$, where n depends on PI, it follows that:

$$\gamma_{ref} \propto p'^{1-n} \tag{3}$$

Eq.(3) clarifies the reason why the $G/G_0(\gamma)$ curve strongly depends on the mean effective stress in cohesionless soils ($n = 0.5$), while it is substantially independent of p' in high plasticity soils ($n \approx 1$). Moreover, Eq.(3) clarifies the close connection between G, G_0 and τ_{lim}, implying that the effects of p' and PI on G/G_0 are correlated with those on G_0 and τ_{lim}. As a result, these parameters cannot be specified independently of each other.

3 SIMPLE CONSTITUTIVE SOIL MODELS

In the light of the results presented in the previous section, τ_{lim} turns out to be a key ingredient both to limit the maximum shear stress that can be applied to the soil (large strains), and to describe the dependence of the nonlinear soil properties on p' and PI (medium strains). Moreover, the classical hyperbolic model clearly retains all the constitutive ingredients necessary to catch, at least qualitatively, the mechanical behaviour of soils under cyclic loadings. However,

as already observed by Hardin and Drnevich (1972), additional parameters are required to provide a quantitative description of the actual soil behaviour.

In this section, two nonlinear models are presented, capable of describing the main features of the soil behaviour under cyclic loading with a simple constitutive approach. The models are completely defined by two equations, describing the stress-strain relationship along the backbone and the symmetric unloading-reloading cycles, respectively. In the

3.1 *The DM model*

The first model (hereafter the DM model) combines the functional form proposed by Davidenkov (1938) for the backbone, with the inversion rule suggested by Muravskii (2005). Specifically, $\Phi(\gamma)$ is given by:

$$\Phi(\lambda) = \begin{cases} \lambda(a - b|\lambda|^n) & |\lambda| \le \lambda_L \\ sign(\lambda) \cdot \tau_{lim} & |\lambda| > \lambda_L \end{cases} \tag{4}$$

where γ_L is the shear strain corresponding to which the strength is attained. Accordingly, $\Phi(\gamma)$ must satisfy the following constraints:

$$\Phi'(0) = G_0 \tag{5.1}$$

$$\Phi'(\gamma_L) = 0 \tag{5.2}$$

$$\Phi(\gamma_L) = \tau_{lim} \tag{5.3}$$

After simple manipulation, coefficients *a, b* and *n* in Eq. (4) can be written as:

$$a = G_0 \tag{6.1}$$

$$b = G_0 \frac{\left(1 - \gamma_{ref}/\gamma_L\right)}{\gamma_L^n} \tag{6.2}$$

$$n = \frac{\gamma_{ref}/\gamma_L}{1 - \gamma_{ref}/\gamma_L} \tag{6.3}$$

where $\gamma_{ref} = \tau_{lim}/G_0$, and the corresponding shear modulus degradation curve is:

$$G/G_0(\gamma) = \begin{cases} 1 - (\gamma/\gamma_L)^n\left(1 - \gamma_{ref}/\gamma_L\right) & \gamma \le \gamma_L \\ \gamma_{ref}/\gamma & \gamma > \gamma_L \end{cases} \tag{7}$$

As a result, the backbone is completely defined by three parameters, *i.e.*: the small strain shear modulus, G_0; the shear strength, τ_{lim}; and the shear strain γ_L, which can be viewed as a best fitting parameter, to be calibrated based on a given set of G/G_0 experimental data. In other words, as the classical hyperbolic model, the MD model also takes into account the dependence of the nonlinear soil properties on p' and PI and a finite value of the shear strength, but retaining more flexibility to have a better fit with the experimental G/G_0 data.

As an example, Figure 1 shows (a) the backbone and (b) the shear modulus degradation curve predicted by the DM model for three different values of γ_L. The shear strength is always attained for a finite value of the shear strain, γ_L, which govern also the shape of the $G/G_0(\gamma)$ curve.

The unloading-reloading rule suggested by Muravskii (2005) is adopted for the DM model, defined as:

$$\tau - \tau_r = \Psi(u) = \Psi(\gamma - \gamma_r) \tag{8}$$

where $\Psi(u)$ must satisfy the following conditions:

$$\Psi(0) = 0 \tag{9.1}$$

$$\Psi'(0) = \Phi'(0) \tag{9.2}$$

$$\Psi(2\gamma_r) = 2\tau_r \tag{9.3}$$

$$\Psi'(2\gamma_r) = \Phi'(\gamma_r) \tag{9.4}$$

Specifically, if $\Psi(u)$ has the same functional form of the backbone, it is:

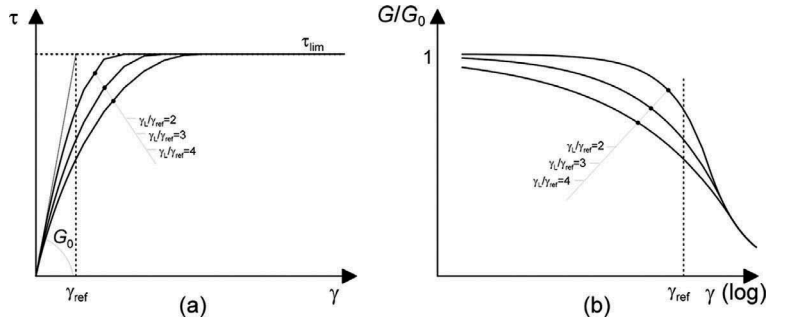

Figure 1. DM model: (a) backbone and (b) shear modulus degradation curve.

$$\Psi(u) = u\left(a^* - b^*|u|^{n^*}\right) \tag{10}$$

where, in order to fulfil Eqs. (9), it must be:

$$a^* = G_0 \tag{11.1}$$

$$b^* = \frac{a^*\gamma_r - \tau_r}{\gamma_r|2\gamma_r|^{n^*}} \tag{11.2}$$

$$n^* = \frac{\tau_r - \gamma_r\Phi'(-\gamma_r)}{a^*\gamma_r - \tau_r} \tag{11.3}$$

The Muravskii's unloading-reloading rule does not require the introduction of any other material parameter. Moreover, as shown by Muravskii (2005), it reduces the implied hysteretic damping with respect to the classical second Masing's rule.

3.2 *The MHD model*

The second model discussed in this paper (hereafter the MHD model) combines the hyperbolic functional form originally introduced by Hardin and Drnevich (1972) for the backbone with the unloading-reloading rule suggested by Phillips and Hashash (2009).

Following Hardin and Drnevich (1972), $\Phi(\gamma)$ is given by:

$$\Phi(\gamma) = \frac{G_0\gamma}{1 + \frac{\gamma}{\gamma_{ref}}\left[1 + aexp\left(-b\frac{\gamma}{\gamma_{ref}}\right)\right]} \tag{12}$$

where a and b are two model parameters, and $\gamma_{ref} = \tau_{lim}/G_0$. The corresponding shear modulus degradation curve is:

$$G/G_0(\gamma) = \frac{1}{1 + \frac{\gamma}{\gamma_{ref}}\left[1 + a\,\exp\left(-b\frac{\gamma}{\gamma_{ref}}\right)\right]} \tag{13}$$

According to Eq.(13), the constants a and b govern the model behaviour in the medium strain range. Specifically, b must be positive in order to recover the asymptotic condition of $\tau = \tau_{lim}$ for $\gamma \rightarrow \infty$. On the contrary, a can assume also negative values. The practical significance of a is clear from Figure 2, showing a schematic representation of the model predictions for three different values of a ($b = 1$). Negative values of a shift the $G/G_0(\gamma)$ curve to the right with respect to the case $a = 0$, thus increasing the "linearity threshold" of the model. The opposite trend is obtained for $a > 0$.

Different values of a and b for clean sands and cohesive soils are computed by Hardin and Drnevich (1972), with a ranging from -0.5 to 1.5 and b from 0.16 to 1.3. More recently, Wichtmann and Triantafyllidis (2013) showed that a good prediction of the $G/G_0(\gamma)$ curve for quartz sands can be achieved assuming $b = 1$ and linking a to the uniformity coefficient.

The unloading-reloading rule suggested by Phillips and Hashash (2009) is adopted for the MHD model, defined as:

$$\tau - \tau_r = 2\alpha(\gamma_m)\Phi\left(\frac{\gamma - \gamma_r}{2}\right) + [1 - \alpha(\gamma_m)]\Psi(\gamma - \gamma_r) \tag{14}$$

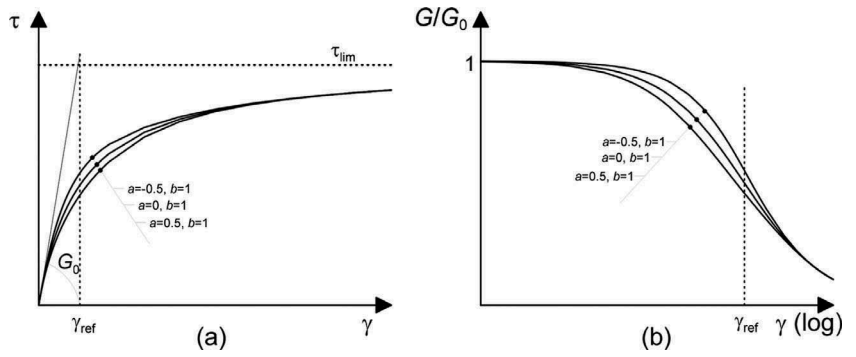

Figure 2. MHD model: (a) backbone and (b) shear modulus degradation curve.

where τ_r and γ_r are the reversal shear stress and strain respectively, γ_m is the current maximum shear strain ($\gamma_m = \gamma_r$ for symmetric cyclic loading), and the function $\Psi(\gamma)$ is given by:

$$\Psi(\gamma) = \frac{G_0\gamma}{1 + \frac{\gamma_m}{\gamma_{ref}}\left[1 + aexp\left(-b\frac{\gamma_m}{\gamma_{ref}}\right)\right]} \tag{15}$$

By integrating Eq. (14) over one symmetric cycle, it follows that the coefficient $\alpha(\gamma_r)$ can be viewed as a reduction factor for damping, corresponding to:

$$\alpha(\gamma_r) = \frac{D^{PH}(\gamma_r)}{D^{M}(\gamma_r)} \tag{16}$$

where $D^{M}(\gamma_r)$ and $D^{PH}(\gamma_r)$ are the damping values resulting from the application of the second original Masing's rule and Eq.(14), respectively. Specifically, the expression used for $\alpha(\gamma_m)$ is:

$$\alpha(\gamma_m) = 1 - c\left[1 - \frac{G(\gamma_m)}{G_0}\right]^d \tag{17}$$

which is only a slight simplification with respect to that provided by Phillips & Hashash (2009), where c and d are model constants.

The calibration procedure for c and d, based on a given set of experimental data, is detailed by Phillips & Hashash (2009). Purely indicative values of c and d, as referring to the standard hyperbolic model and a slightly different version of Eq.(17), can be found in the same reference, based on the analysis of various tested soils.

4 VALIDATION OF THE MHD MODEL

Based on a thorough comparison with available experimental data and empirical relationships, it was found that the MHD model provides always a better agreement with the observed soil behaviour in terms of $G/G_0(\gamma)$ curves. Therefore, only the MHD model will be considered for further validation.

4.1 *Calibration of model parameters*

The MHD model is defined by six parameters (τ_{lim}, G_0, *a, b, c* and *d*). As already observed, *a* and *b* control the shape of the $G/G_0(\gamma)$ curve, making the hyperbolic function more flexible in the medium strain range, while *c* and *d* govern the $D(\gamma)$ curve, reducing the hysteretic damping implied in the standard Masing's rules. These four parameters are assumed to depend solely on intrinsic soil properties.

As far as the calibration of the model parameters is concerned, G_0 and τ_{lim}, can be estimated from standard in situ tests (SPT, CPT, V_S measurements). The remaining constants (*a, b, c* and *d*) can be viewed as curve-fitting parameters. As depending solely on the nature of the soil, they can be calibrated based either on the experimental data from one single cyclic

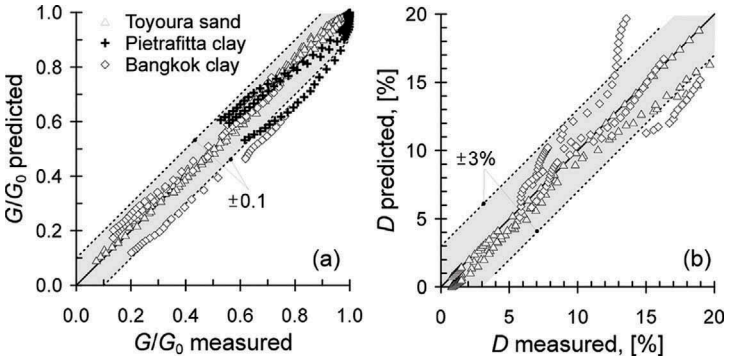

Figure 3. Comparison between predicted and measured (a) G/G_0 and (b) D values.

laboratory test (RC, TS or simple shear), carried out at a given value of p', or from literature regression models, referring again to a given value of p'.

4.2 *Comparison with experimental data*

The experimental data referring to three well-documented soils (Toyoura sand, Pietrafitta clay and Bangkok soft clay) were used to verify the predictive capabilities of the MHD model. The comparison between model predictions and experimental data serves primarily to demonstrate the ability of the model to predict the $G/G_0(\gamma)$ and $D(\gamma)$ curves in the medium strange range, while maintaining naturally a good prediction of the soil shear strength.

The experimental data and the validation stage are thoroughly discussed in Conti *et al.* (2019). A summary of the results obtained is shown in Figure 3, where the predicted values of G/G_0, D and τ/τ_{lim} are plotted against the corresponding experimental or empirical data. As far as G/G_0 and D are concerned, most of the data points lie close to the bisecting line, confirming that the model provides a good description of the expected soil behaviour in the small-to-medium strain range, in terms of nonlinearity and damping. Specifically, the difference between measured and predicted G/G_0 data is less than 0.1 in 95% of the cases. The trend is more dispersed in terms of damping, but still the difference between measured and predicted data is less than 4% in 90% of the cases.

The larger number of curve-fitting parameters makes more advanced nonlinear models (see *e.g.* Groholski *et al.*, 2016), more accurate in reproducing the experimental $D(\gamma)$ curves. However, taking into consideration that a small amount of damping, in the order of 1–4 %, is often added to the laboratory-based values to reduce the high-frequency amplification in numerical seismic response analyses (Yee *et al.*, 2013; Conti *et al.*, 2014), a difference of 4% between measured and predicted data does indicate a satisfactory prediction of the proposed model.

5 APPLICATION TO A CASE STUDY

The performance of the proposed model in nonlinear seismic site response analyses is verified with reference to the well-characterised Eastern Napoli site in Italy (Vinale, 1988). Figure 4 shows a schematic representation of the stratigraphy, consisting of made ground (R), overlying volcanic ash (C) and pyroclastic silty sand (cohesionless, Ps, and weakly cemented, Pc, pozzolana), alternating with alluvial soils (peat, T, and sand, S). Figure 4 also shows the shear wave velocity profiles, together with the assumed modulus reduction and damping curves, considered as representative of confining pressures in the range of 100–250 kPa. Table 1 summarises the relevant physical and mechanical properties of the soil layers, together with the constitutive parameters adopted for the MHD model.

In order to highlight the importance of considering both nonlinearity and strength as key constitutive ingredients, a further comparison is provided with the predictions of the

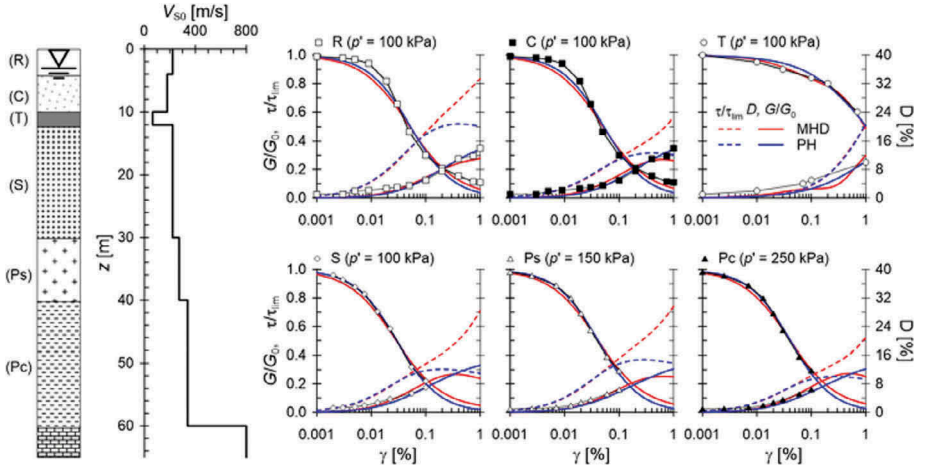

Figure 4. East Naples site: stratigraphy, shear wave velocity profile and $G/G_0(\gamma)$ and $D(\gamma)$ curves. Calibration of MHD and PH models.

Table 1. Physical/mechanical properties and constitutive parameters (MHD) for the East Napoli site soils.

layer	γ [kN/m^3]	V_{S0} [m/s]	Ø [°]	c' [kPa]	OCR [-]	a [-]	b [-]	c [-]	d [-]
R	15	222	28	10	1.0	0.49	0.1	0.83	0.96
C	14	179	28	10	2.3	1.47	0.1	0.78	0.94
T	12	65	30	0	1.0	2.74	10.0	0.96	3.41
S	17	222	36	0	1.0	1.44	0.1	0.74	0.84
Ps	15	273	37	0	2.3	0.95	0.1	0.78	0.88
Pc	15	340	28	100	3.0	1.86	0.1	0.74	0.86

widely-used hyperbolic model, as modified by Phillips and Hashash (2009) (hereafter the PH model), not including explicitly τ_{lim} in the formulation of the backbone.

The results of the calibration procedure are also illustrated in Figure 4, indicating a general good agreement between target data and models' predictions, in terms of modulus reduction and damping curves. However, the PH model under-predicts substantially the expected soil shear strength, with the only exception of the peat layer (T).

Twenty natural strong earthquakes were considered in this study, selected based on a site specific hazard analysis, for a return period of 10000 years (Iervolino *et al.*, 2017). The above signals were applied as a bedrock acceleration time history at the bottom nodes of the 1D soil column.

The main results of the site response analyses, in terms of mean values among all the applied earthquakes, are summarised in Figure 5, showing: the profiles of (a) maximum shear strain (γ_{max}), (b) maximum acceleration (a_{max}) and (c) maximum shear stress (τ_{max}) mobilised in the soil column; and (d) the ratio between the 5% elastic response spectra of surface and input accelerations. As far as the MHD model is concerned (red lines), a concentration of shear strain in the soft peaty layer induces locally a partial mobilisation of the soil shear strength and an attenuation of the accelerations propagating upwards. This effect is even more evident by inspection of the ratio of elastic response spectra, where the high-frequency components of the input signals ($T < 0.5$ s) are de-amplified as a result of the filtering action of the peat layer. On the other hand, amplification phenomena occur at higher periods (T = 0.5–2 s), due to the overall dynamic response of the soil deposit (the filled region in the figure indicates the range of the first two natural frequencies of the soil deposit, taking into account possible nonlinear effects).

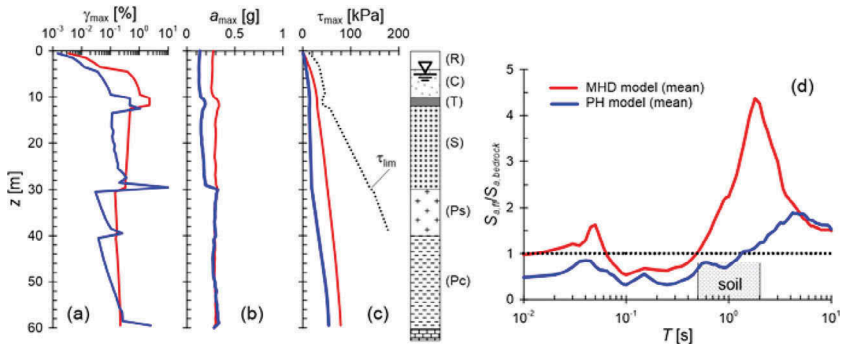

Figure 5. Site response analysis at East Naples site. Profiles of (a) maximum shear strain, (b) maximum acceleration and (c) maximum shear stress mobilised in the soil column, together with (c) the ratio between surface and bedrock elastic response spectra.

As far as the PH model is concerned (blue lines), the under-prediction of the soil shear strength leads to an unrealistic concentration of shear strains at the contact between the loose pyroclastic layer, Ps, and the adjacent layers. This result induces an unrealistic reduction of the surface accelerations, which turn out to be damped in the whole frequency range.

This case study is paradigmatic of the possible misinterpretation of amplification phenomena when τ_{lim} is not taken into account properly, even in cases where the soil shear strength is actually far from being mobilised. As a matter of fact, the apparent localization of shear strains predicted by the PH model within the deeper soil layers (S, Ps, Pc) is merely due to an erroneous under-prediction of the soil shear strength. On the contrary, as predicted by the MHD model, the deeper soil layers are actually far from reaching failure under the earthquake-induced shear stresses.

6 CONCLUSIONS

In this work, a simple and easy to calibrate constitutive soil model was proposed, capable of describing the observed soil behaviour not only in the small-to-medium strain range, where the confining-stress dependency of nonlinear soil properties is the key feature, but also at large strains, where a possible attainment of the shear strength is expected.

This basic idea of using τ_{lim} as a constitutive ingredient not only to limit the allowable shear stress, but also to describe the dependence of the nonlinear soil properties on p′ and PI, has three main practical implications:

1. the model parameters can be significantly reduced, without losing accuracy in the model predictions;
2. the proposed model takes into account implicitly the confining-stress dependency of the $G/G_0(\gamma)$ and $D(\gamma)$ curves, without further need of additional parameters or equations;
3. by default, the predicted shear modulus reduction and damping curves turn out to be compatible with site-specific shear strength and shear wave velocity profiles.

From a practical point of view, these considerations make the proposed model very attractive when performing 1D site response analysis in standard design practice, where the simplicity of the constitutive equation and the limited number of parameters are by all means key ingredients.

REFERENCES

Conti R., Viggiani G. M. B., Perugini F. 2014. Numerical modelling of centrifuge dynamic tests of circular tunnels in dry sand. *Acta Geotechnica*, 9(4),597–612.

Conti R., Licata V., Angelini M. 2019. Nonlinearity and strength in 1D site response analyses: a simple constitutive approach. Submitted to *Géotechnique*.

Groholski, D., Hashash, Y.M.A., Kim, B., Musgrove, M., Harmon, J., Stewart, J. 2016. Simplified Model for Small-Strain Nonlinearity and Strength in 1D Seismic Site Response Analysis. J. *Geotech. Geoenvir. Eng*., 142(9), doi:10.1061/(ASCE)GT.1943-5606.0001496.

Davidenkov, N.N. 1938. Energy dissipation in vibrations. J. *Tech. Phys*., 8 (6),(in Russian).

Hardin, B.O., Drnevich, V.P. 1972. Shear modulus and damping in soils: Design equations and curves. *J. Soil Mech. Found. Eng. Div*., 98(SM7), 667–692.

Iervolino, I., Spillatura, A., Bazzurro, P. 2017. RINTC project: Assessing the (implicit) seismic risk of code-conforming structures in Italy. 6th ECCOMAS thematic conference on computational methods in structural dynamics and earthquake engineering (COMPDYN 2017), Rhodes, Greece

Kishida, T. 2017. Comparison and Correction of Modulus Reduction Models for Clays and Silts. *J. Geotech. Geoenv. Eng*., 143(4), doi:10.1061/(ASCE)GT.1943-5606.0001627.

Kondner, R.L., Zelasko, J.S. 1963. Hyperbolic stress-strain formulation of sands. 2nd pan American Conf. on Soil Mechanics and Foundation Engineering, Associação Brasileira de Mecânica dos Solos, São Paulo, Brazil.

Muravskii, G. 2005. On description of hysteretic behaviour of materials. *Int. J. Solid. Str*., 42, 2625–2644.

Phillips, C., and Hashash, Y.M.A. 2009. Damping formulation for nonlinear 1D site response analyses. *Soil Dyn. Earthquake Eng*., 29(7),1143–1158.

Régnier, J., Bonilla L., et al 2018. PRENOLIN: International Benchmark on 1D Nonlinear Site-Response Analysis - Validation Phase Exercise. *Bull. Seismol. Soc. Am*., DOI: 10.1785/0120170210.

Vinale, F. 1988. Caratterizzazione del sottosuolo di un'area campione di Napoli ai fini di una microzonazione sismica. *Rivista Italiana di Geotecnica*, 22 (2),77–100(in Italian).

Wichtmann T., Triantafyllidis T. 2013. Effect of uniformity coefficient on G/Gmax and damping ratio of uniform to well graded quartz sands. *J. Geotech. Geoenviron. Eng*., 139(1),59–72.

Yee, E., Stewart, J.P., Tokimatsu, K. 2013. Elastic and large-strain nonlinear seismic site response from analysis of vertical array recordings. *J. Geotech. Geoenviron. Eng*., 139(10),1789–1801.